# Probing protein dynamics in neuronal nitric oxide synthase by quantitative cross-linking mass spectrometry

| | |
|---|---|
| Journal: | *Biochemistry* |
| Manuscript ID | bi-2023-00245w.R2 |
| Manuscript Type: | Communication |
| Date Submitted by the Author: | 06-Jul-2023 |
| Complete List of Authors: | Jiang, Ting ; University of New Mexico College of Arts and Sciences<br>Wan, Guanghua; University of New Mexico, College of Pharmacy<br>Zhang, Haikun; University of New Mexico, College of Pharmacy<br>Gyawali, Yadav; University of New Mexico Health Sciences Center<br>Underbakke, Eric; Iowa State University, Roy J. Carver Dept. Biochemistry, Biophysics, and Molecular Biology<br>Feng, Changjian; University of New Mexico, College of Pharmacy |
| | |

# Probing protein dynamics in neuronal nitric oxide synthase by quantitative cross-linking mass spectrometry

*Ting Jiang [1, ‡], Guanghua Wan [1, ‡], Haikun Zhang [1], Yadav Prasad Gyawali [1], Eric S. Underbakke [2], Changjian Feng [1, *]*

[1] College of Pharmacy, University of New Mexico, Albuquerque, NM 87131

[2] Roy J. Carver Department of Biochemistry, Biophysics and Molecular Biology, Iowa State University, Ames, IA 50011

## ABSTRACT

Nitric oxide synthase (NOS) is responsible for biosynthesis of nitric oxide (NO), an important signaling molecule controlling diverse physiological processes such as neurotransmission and vasodilation. Neuronal NOS (nNOS) is a calmodulin (CaM)-controlled enzyme. In the absence of CaM, several nNOS-unique control elements, along with $NADP^+$ binding, suppress electron transfer across the NOS domains. CaM binding relieves the inhibitory factors to promote the electron transport required for NO production. The regulatory dynamics of nNOS control elements are critical to governing NO signaling, yet mechanistic questions remain because the intrinsic dynamics of NOS thwart traditional structural biology approaches. Here, we employ cross-linking mass spectrometry (XL MS) to probe regulatory dynamics in nNOS, focusing on the CaM-responsive control elements. Quantitative cross-linking revealed conformational changes differentiating the nNOS reductase (nNOSred) alone, nNOSred with $NADP^+$, nNOS-CaM, and nNOS-CaM with $NADP^+$. We observed distinct effects of CaM vs. $NADP^+$ on cross-linking patterns in nNOSred. CaM induces striking global changes while the impact of $NADP^+$ is primarily localized to the NADPH-binding subdomain. Moreover, CaM increases the abundance of intra-nNOS cross-links that are related to the formation of the inter-CaM-nNOS cross-links. These XL MS results demonstrate that CaM and $NADP^+$ site-specifically alter the nNOS conformational landscape.

NOS is a homodimeric enzyme, with its subunit composed of an oxygenase domain and a reductase domain that contains NADPH-, FAD- and FMN-binding subdomains (Figure 1A). The $Ca^{2+}$-sensing protein CaM activates NO biosynthesis by binding to the linker connecting the oxygenase and reductase domains.

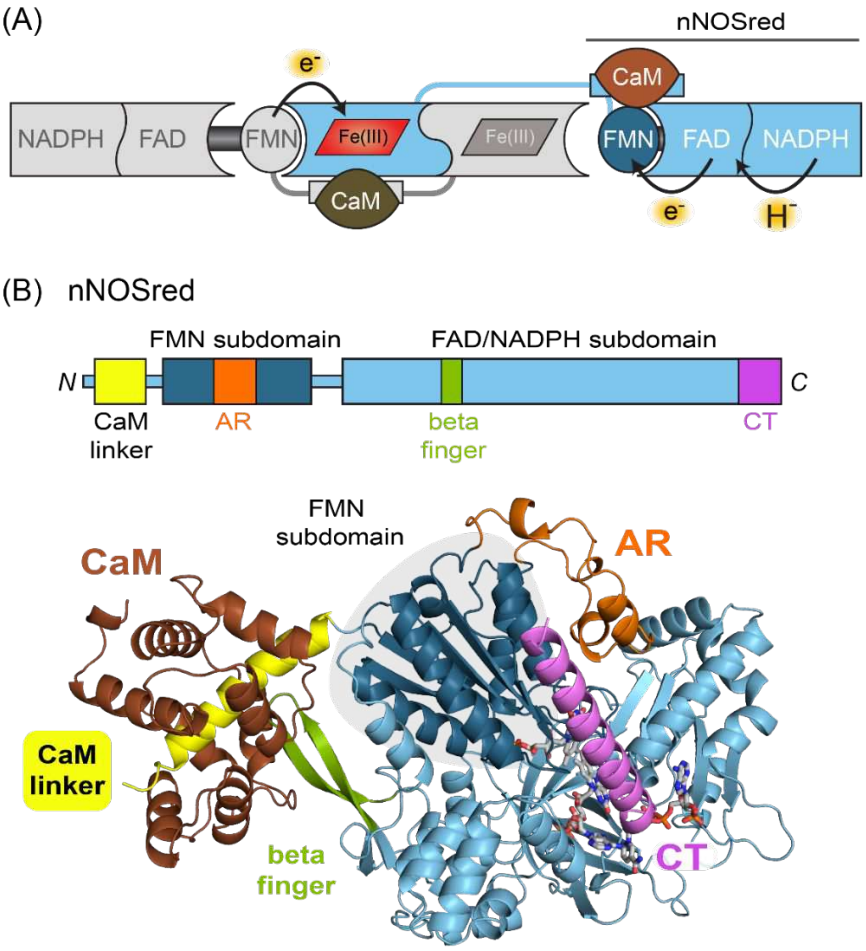


**Figure 1. A.** Mammalian NOS domain organization and electron flux through the protein. **B.** A top AlphaFold Multimer[1] model of CaM-bound nNOSred. Control of the electron transport

processes in nNOS by CaM involves several intrinsic control elements: the CaM binding linker, an autoregulatory (AR) insert within the FMN subdomain, a β finger, and a C-terminal tail (CT).[2] Recent single particle electron microscopy (EM) studies[3, 4] revealed the general architecture of the NOS enzyme, in which the relatively rigid subdomain modules are connected by flexible tethers. NOS adopts conformations enabled by the flexible tethers and populates a continuum of free and docked states.[4, 5] Given the importance of large-scale rearrangements of the NOS domains for NO production, defining how conformational dynamics are tuned by CaM and control elements is critical for understanding the regulation of NOS. The reported high resolution structures of isolated NOS domains capture valuable views of static states. However, new approaches are needed to assess the range of conformational dynamics involved in the NOS regulation and catalysis.

Cross-linking mass spectrometry (XL MS) is a solution-based approach that can identify residues in spatial proximity, providing medium-resolution information on relative domain positions and orientations.[6] In this work, we chose to study the rat nNOSred construct with residues 695-1429 that encompass the NADPH-, FAD-, and FMN-subdomains, as well as the CaM-binding linker (Figure 1B).[7] The nNOSred protein is monomeric in solution yet fully active in supporting electron transport across the domains. Indeed, our purified nNOSred protein exhibited over 8-fold increase in cytochrome (cyt.) *c* reduction activities upon CaM binding (Figure S2). Steady-state cyt. *c* reduction is a measure of electron transport through the entire reductase domain because cyt. *c* is

reduced exclusively by the FMN cofactor.[8] Importantly, the functionality of nNOSred as a monomer is advantageous for XL MS, circumventing the challenges of discerning inter- vs. intra-subunit cross-links.

To assess structural changes associated with a range of regulatory states, we aimed to obtain quantitative MS data to compare relative abundances of key intra- and inter-protein cross-links with or without $NADP^+$ and CaM. Notably, $NADP^+$ has a physiologically relevant regulatory role.[9] In the absence of CaM, NADP(H) binding is thought to lock the nNOS reductase domain in a conformation that restricts motion of the FMN subdomain;[10] this "conformational lock" effect is proposed to be relieved by CaM binding.[9]

We selected an MS-cleavable cross-linker of primary amines, disuccinimidyl dibutyric urea (DSBU).[11] To minimize kinetically-trapped higher-order crosslinks between complexes, we optimized the cross-linking reaction conditions for nNOSred until a distinct species consistent with CaM- nNOSred heterocomplex appeared as a unique gel-shifted band by SDS-PAGE, and the nNOS-alone band was also evident (Figure S3). The two bands in each lane were then excised, in-gel digested with trypsin and LysC proteases, and subjected to the LC-MS/MS using data-dependent acquisition (DDA) with stepped higher-energy collisional dissociation (HCD).[12]

We profiled the cross-links in each excised gel band and identified a total of 71 unique intra-nNOS cross-links from the lower molecular weight (MW) band samples (Table S1); three reaction replicates were analyzed for each condition. Figure S6 illustrates the intra cross-links in a nNOSred-alone sample. We observed cross-links of the lysine residues at the CaM-binding linker (K732, K733, K739, K743), AR (K842, K856), β hairpin (K1080), NADP(H) binding subdomain (K1320), and CT (K1420); Table S1. We then mapped these cross-links to a structural model generated by AlphaFold 2,[13] as the CaM-free nNOSred crystal structure (pdb ID 1TLL) does not resolve all portions of the AR and CT elements. Figure S7A shows the intra-links mapped to a top AlphaFold model. Of the 48 total crosslinking, 36 mapped within the Cα-Cα Euclidean distance threshold of the DSBU-linked lysines (40 Å) (Table S2) and thus appear in general agreement with the AlphaFold model. We chose a Cα–Cα distance threshold of 40 Å for the lysine pairs to account for the conformational flexibility of the nNOS protein; this distance was also used in other studies.[14]

The other 12 cross-links are outside the DSBU distance range, many of which are at the AR and CT sites (e.g., K842, K856, K1420; Figure 2A). The extra-long-range cross-links indicate that these regions are highly dynamic, sampling a range of conformational distances. Indeed, the apparent conformational freedom of AR and CT is consistent with the poor resolution of these regions in the reported structure.[10] The confidence of AlphaFold prediction for AR and CT regions is also lower than the well-folded rigid FMN and FAD domains (Figure S7B). We recognize that if the domains cannot reasonably reach each other, the underlying assumption that the cross-links are intramolecular and from a properly folded protein may come into doubt. We point to the use

of gel extractions (Figure S3) to indicate that the observed crosslinks derive from intra- rather than inter-molecular crosslinks. We are aware that a subpopulation of unfolded protein could generate unrealistically long-range crosslinks. However, our cyt. *c* reduction activity assays (Figure S2) indicate that the specific activity is consistent with a well-folded, functional nNOSred. In addition, longer range crosslinks are commonly observed,[15] which can be an indication of protein dynamics and conformational flexibility in those regions. Indeed, the nNOS electron shuttling mechanism is dependent on a high degree of interdomain mobility,[4] and the observed crosslinks are consistent with such mechanism.

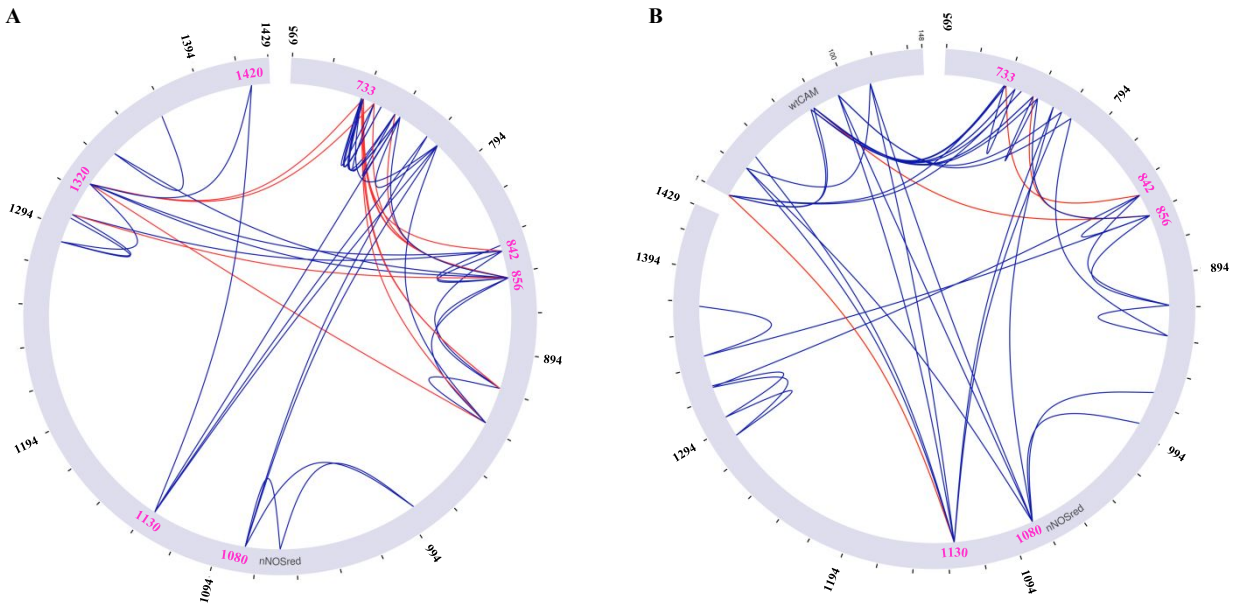


**Figure 2.** Circular cross-link map depicting the interconnectivity in (A) nNOSred protein and (B) CaM-nNOSred sample. Cross-links were mapped to an AlphaFold model representing a static snapshot of nNOSred without (A) or with (B) bound CaM. Cross-links with mapped Cα−Cα

distances below and above 40 Å threshold are shown in blue and red, respectively. Selected residues including those at the CaM-binding linker (K733), AR (K842, K856), β finger (K1080), and CT (K1420) are labeled in magenta.

For the CaM-nNOSred complex, we observed 24 unique inter CaM-nNOSred links from the higher MW CaM-nNOSred band samples (Figure S8 and Table S3). As expected, we detected several cross-links at the canonical CaM-binding linker in nNOS (K732, K733, K739, K743); these cross-links connect with CaM, and only the nNOS residues are listed in the parentheses. Excitingly, we also observed the AR (K856) and β-finger (K1080) regions cross-linked with CaM sites. The β-finger and AR were proposed to be near the bound CaM,[16] and interact with CaM,[17] respectively, and our XL MS data provide, for the first time, direct experimental distance range information in supporting their relatively close proximity. These results corroborate the impact on these regions reflected by previous HDX MS data comparing the CaM-free and CaM-bound nNOS.[18] CaM-binding induces increased conformational dynamics at the β finger region in the full-length nNOS.[18] Upon CaM binding to nNOS, the AR and CT are not directly impacted, but pockets of the FMN and NADPH subdomains enveloping the AR and CT are perturbed.[18] Notably, cross-linking provides a distinct and critical dimension of structural data (i.e., distance restraints) that HDX MS cannot technically distinguish. Importantly, the observed cross-linking pairs can be

mapped to an inter-protein NOS-CaM complex structural model by AlphaFold (Figure S9):[13] the distances between the lysine residues are listed in Table S4, where most of the inter-links are mapped within the distance constraint (Figure 2B). One cross-link, K856(nNOS)-K77(CaM) sampling the nNOS AR motif, exceeds the DSBU distance threshold when mapped to the model (Figure 2B), indicating that the AR region is more dynamic than the other sites. The experimental cross-link provides actual distance restraint, and the model needs to be updated to reflect the apparent dynamics, as the distance comes out of mapping to the static model generated from a truncation packed in a crystal lattice.

To further assess regulatory factor-dependent structural changes in nNOS, we obtained quantitative MS data to compare relative abundances of individual cross-links in the $NADP^+$-bound vs. -free, and/or CaM-bound vs. -free nNOSred samples. The inclusion list and Skyline library for our parallel reaction monitoring (PRM) experiments were built by combining the identified cross-linked peptides from all the abovementioned DDA runs. Representative PRM results for the intra-cross-links and inter CaM-NOS cross-links are illustrated in Figures S10 and S11, respectively (Tables S5-S7). For such relative quantitation, each cross-linked peptide pair is independently targeted for PRM analysis, and relative ratios can be calculated from the total PRM transition chromatographic peak areas. The heatmap in Figure 3 illustrates the quantified intra-cross-linked peptide pairs under the sample conditions.

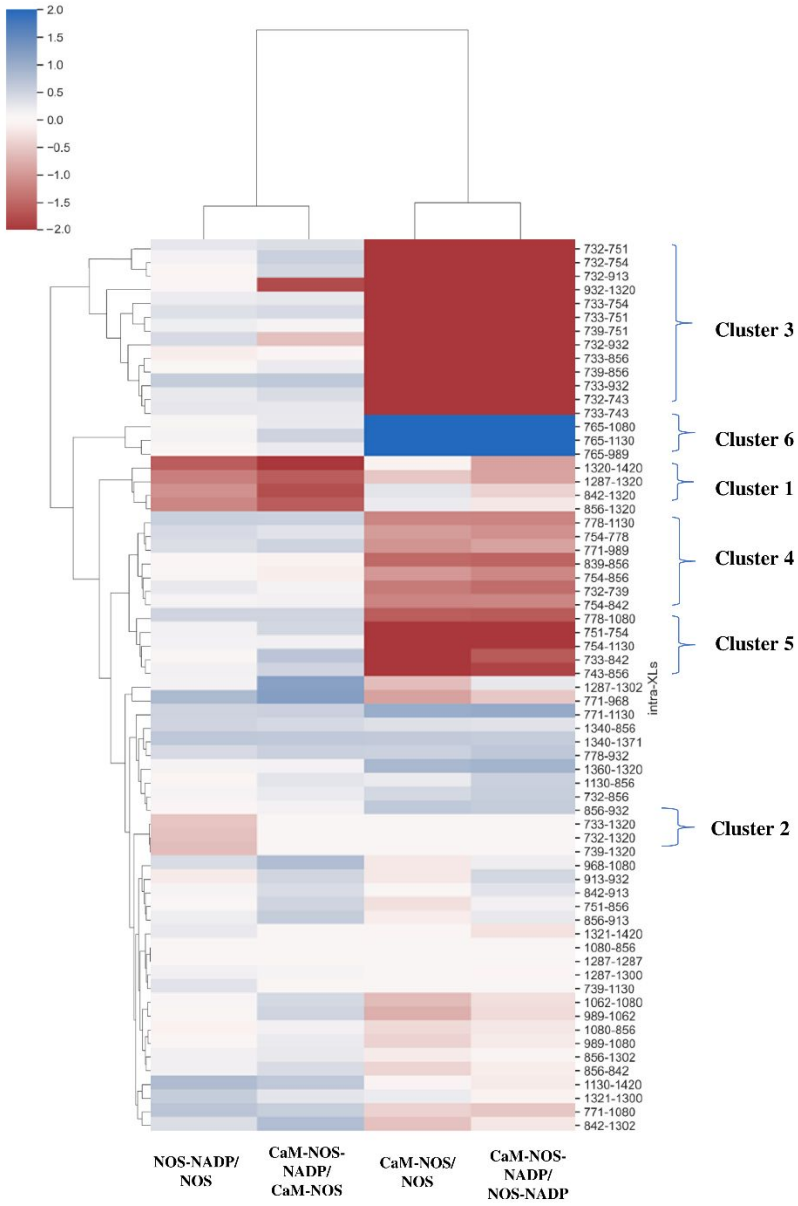


**Figure 3.** Hierarchical clustering heat map comparing the changes in abundance of the intra-nNOSred cross-links between samples NOS-NADP (nNOSred with added $NADP^+$), NOS (nNOSred without $NADP^+$), CaM-NOS-NADP (CaM-bound nNOSred with added $NADP^+$), and CaM-NOS (CaM-bound nNOSred without $NADP^+$). The changes relative to the $NADP^+$- or CaM-

free state are represented by the specified ratios, with their $\log_2$ values displayed by the color scale. The heatmap was generated by the Python Seaborn library.

We first examined the effects of $NADP^+$ ligand binding on the intra-nNOS cross-links. $NADP^+$ was added to a final concentration of 150 μM, a 25-fold excess over the reported dissociation constant (6 ± 1 μM),[19] resulting in > 98 % $NADP^+$-bound nNOSred form. In the CaM-free nNOS samples, there are 4 cross-links decreased by over 2-fold in their abundance upon $NADP^+$ addition (Cluster 1 in Figure 3; Table S5), all of which are between the K1320 site in the NADP(H) binding subdomain and AR (K842), AR (K856), CT (K1420), or K1287. These CaM-responsive control elements thus appear to respond to $NADP^+$ binding in the absence of CaM and alter their conformational populations so that fewer of them may sample the conformational space adjacent to K1320. Other cross-links were not substantially impacted by $NADP^+$ binding. $NADP^+$ binding to nNOS thus site specifically alters the local conformational landscape at the CaM-responsive control elements.

Additionally, abundances of three cross-links between the $NADP^+$ binding pocket (K1320) and CaM-binding linker (K732, K733) were decreased by ~1.5-fold upon addition of $NADP^+$ (Cluster 2 in Figure 3). In the samples of CaM-nNOS with or without added $NADP^+$, these intra-cross-links between K1320 and the CaM-binding linker (K732, K739) were not even observed (Cluster 2 in Figure 3); several other intra-cross-links of K1320 with K842 or K852 (AR region) were also absent. Thus, CaM significantly alters the effect of $NADP^+$ ligand on the cross-links at the K1320 site. HDX-MS work demonstrates that CaM binding to the linker causes notable allosteric conformational changes in the linker and the AR regions,[18] and therefore more dramatic changes in their relative positioning are expected to result in decreased cross-linking efficiency.

We next examined the effects of CaM-binding on the intra cross-links' intensities (Table S6). Many more cross-links were impacted by CaM than $NADP^+$: the relative abundances of 24 cross-links were decreased by over 2-fold (Clusters 3-5 in Figure 3), the majority of which are at the CaM-responsive control elements: Cluster 3 is mainly of the CaM-binding linker, and Clusters 4-5 include the AR and β finger regions. Moreover, $NADP^+$ does not further enhance the CaM-mediated changes in the intra-cross-links, which is in contrast with the abovementioned effect of CaM on the $NADP^+$-mediated changes. In other words, CaM exhibits a more dominant and global effect on the intra-cross-links than $NADP^+$ does.

We observed a substantial increase in a few pairs shown in Cluster 6 of Figure 3: the intra-nNOS cross-links are between K765 and β finger (K1080), K1130, or K989. These changes are much larger in their magnitude than the other peptides, e.g., the 765-1080 intra-nNOS cross-link is increased over 10-fold by CaM in its intensity (Table S6). Figure 4 illustrates these intra-cross-links with substantially changed abundance, along with the inter-cross-links mediated by the nNOS K1080 and K1130 residues. The adjacent regions in nNOS undergo notable conformational changes upon CaM-binding, which likely bring the nNOS and CaM pairing residues into relatively proximity (< 40 Å), forming the inter NOS-CaM cross-links (1080-115, 1080-94, 1080-30, 1080-21, 1130-115, 1130-94,1130-30).

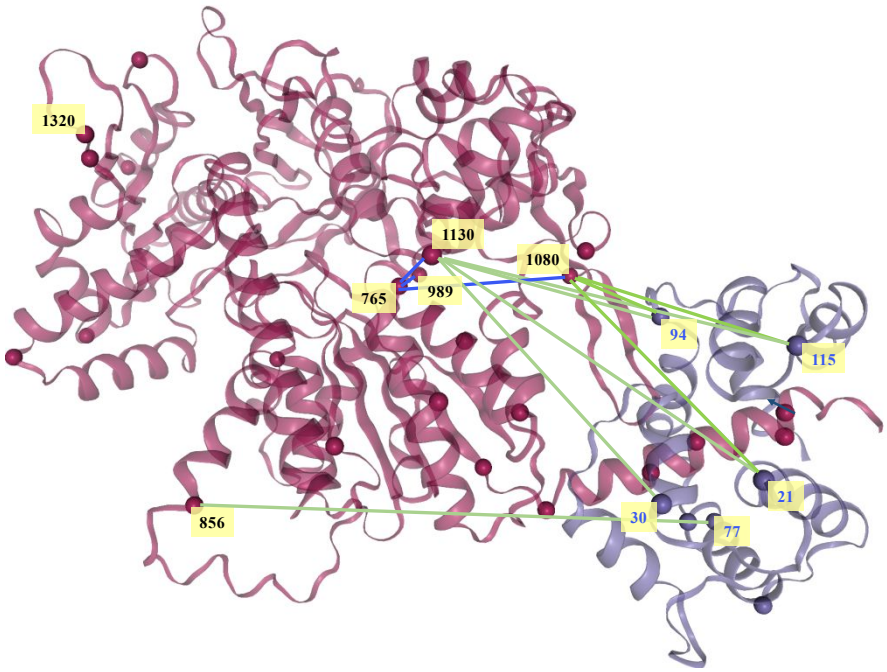


**Figure 4.** The intra-nNOS cross-links exhibiting substantial increases in their abundance upon CaM-binding are mapped on a top AlphaFold Multimer*1* model in blue lines. The inter CaM-nNOS cross-links outside the canonical CaM-binding linker region are shown in green lines. For clarity, cross-links involving the α-helical canonical CaM-binding linker are omitted.

Regarding the effect of $NADP^+$ binding on abundance of the inter NOS-CaM cross-links, the crosslink between nNOS Lys1080 and CaM was ~ 1.75-fold higher upon $NADP^+$ addition; three other inter nNOS-CaM cross-links (1130-115, 754-77, 743-77) showed similar increase in the

range of 1.5 – 1.7 (Table S7). Such change scale (< 2) is often considered as not substantial in quantitative MS. The rest of the inter-cross-links have smaller changes in their PRM intensities. These results indicate that $NADP^+$ binding does not further affect the nNOS conformational distributions, which is in line with its effect on the intra-cross-links.

CaM protein adopts different conformations in the presence or absence of $Ca^{2+}$, which is a critical component of $Ca^{2+}$ responsiveness in many systems. It would be interesting to compare the crosslinking patterns of the nNOSred-CaM complex with or without $Ca^{2+}$. We expect profound conformational changes within the CaM, as NMR studies revealed.[20] However, for the nNOS-CaM interaction, the $Ca^{2+}$-bound conformation is essential for stable nNOS interaction. In fact, we can leverage this $Ca^{2+}$-induced binding and subsequent $Ca^{2+}$ removal for nNOSred enrichment and elution during purification.[7] As such, we don't expect crosslinking would detect $Ca^{2+}$-dependent CaM/nNOS complex rearrangements. Nevertheless, we point to invaluable NMR studies by Guillemette and Dieckmann for $Ca^{2+}$-dependent CaM conformational studies.[21]

In conclusion, this work has provided direct new evidence of proximity changes in the conformations of the CaM-responsive control elements and the $NADP^+$-binding subdomain upon partnering protein (CaM) and ligand ($NADP^+$) binding to nNOS. The results demonstrate that $NADP^+$ and CaM site-specifically alter the conformational landscape. Moreover, CaM-binding induces specific conformational changes within the nNOS reductase domain that correlate well with the formation of CaM-nNOS complex. We speculate that CaM shapes the conformational range of the subdomain motions to enhance electron transport through the entire reductase unit. While it generally remains challenging to pinpoint the structural rationales that result in changed cross-links due to various potential factors (e.g., solvent accessibility, steric factor in reactivity with DSBU), our results clearly demonstrate that CaM- and $NADP^+$-dependent conformational

changes within nNOS can be quantified through PRM-based QXL MS. This provides an exciting new take with foundations in the literature from other very different methods.[18]

## Supporting Information.

Experimental procedures, Tables S1−S7, and Figures S1−S12.

## Accession Codes

Rat nNOS, P29476

## AUTHOR INFORMATION

### Corresponding Author

* Changjian Feng, orcid.org/0000-0003-4542-6497; Email: cfeng@unm.edu

### Author Contributions

‡ T.J and G.W contributed equally.

### Funding Sources

This work is funded by NIH GM133973, P20GM130422, P30ES032755 and NSF 2041692.

REFERENCES

[1] Evans, R., O'Neill, M., Pritzel, A., Antropova, N., Senior, A., Green, T., Žídek, A., Bates, R., Blackwell, S., Yim, J., Ronneberger, O., Bodenstein, S., Zielinski, M., Bridgland, A., Potapenko, A., Cowie, A., Tunyasuvunakool, K., Jain, R., Clancy, E., Kohli, P., Jumper, J., and Hassabis, D. (2022) *bioRxiv*, 2021.2010.2004.463034.

[2] Roman, L. J., Martasek, P., and Masters, B. S. S. (2002) *Chem. Rev. 102*, 1179-1189.

[3] Yokom, A. L., Morishima, Y., Lau, M., Su, M., Glukhova, A., Osawa, Y., and Southworth, D. R. (2014) *J. Biol. Chem. 289*, 16855-16865.

[4] Campbell, M. G., Smith, B. C., Potter, C. S., Carragher, B., and Marletta, M. A. (2014) *Proc Natl Acad Sci U S A 111*, E3614-E3623.

[5] He, Y., Haque, M. M., Stuehr, D. J., and Lu, H. P. (2015) *Proc Natl Acad Sci U S A 112*, 11835-11840.

[6] O'Reilly, F. J., and Rappsilber, J. (2018) *Nat Struct Mol Biol 25*, 1000-1008.

[7] Noble, M. A., Munro, A. W., Rivers, S. L., Robledo, L., Daff, S. N., Yellowlees, L. J., Shimizu, T., Sagami, I., Guillemette, J. G., and Chapman, S. K. (1999) *Biochemistry 38*, 16413-16418.

[8] Matsuda, H., and Iyanagi, T. (1999) *BBA 1473*, 345-355.

[9] Craig, D. H., Chapman, S. K., and Daff, S. (2002) *J. Biol. Chem. 277*, 33987-33994.

[10] Garcin, E. D., Bruns, C. M., Lloyd, S. J., Hosfield, D. J., Tiso, M., Gachhui, R., Stuehr, D. J., Tainer, J. A., and Getzoff, E. D. (2004) *J. Biol. Chem. 279*, 37918-37927.

[11] Matzinger, M., and Mechtler, K. (2021) *J Proteome Res 20*, 78-93.

[12] Stieger, C. E., Doppler, P., and Mechtler, K. (2019) *J Proteome Res 18*, 1363-1370.

[13] Mirdita, M., Schütze, K., Moriwaki, Y., Heo, L., Ovchinnikov, S., and Steinegger, M. (2022) *Nat Meth 19*, 679-682.

[14] Ihling, C. H., Piersimoni, L., Kipping, M., and Sinz, A. (2021) *Anal. Chem. 93*, 11442-11450.

[15] Felker, D., Zhang, H., Bo, Z., Lau, M., Morishima, Y., Schnell, S., and Osawa, Y. (2021) *Biophys. Chem. 274*, 106590.

[16] Jones, R. J., Smith, S. M. E., Gao, Y. T., DeMay, B. S., Mann, K. J., Salerno, K. M., and Salerno, J. C. (2004) *J. Biol. Chem. 279*, 36876-36883.

[17] Salerno, J. C., Harris, D. E., Irizarry, K., Patel, B., Morales, A. J., Smith, S. M. E., Martasek, P., Roman, L. J., Masters, B. S. S., Jones, C. L., Weissman, B. A., Lane, P., Liu, Q., and Gross, S. S. (1997) *J. Biol. Chem. 272*, 29769-29777.

[18] Hanson, Q. M., Carley, J. R., Gilbreath, T. J., Smith, B. C., and Underbakke, E. S. (2018) *J. Mol. Biol. 430*, 935-947.

[19] Konas, D. W., Zhu, K., Sharma, M., Aulak, K. S., Brudvig, G. W., and Stuehr, D. J. (2004) *J. Biol. Chem. 279*, 35412-35425.

[20] Piazza, M., Taiakina, V., Dieckmann, T., and Guillemette, J. G. (2017) *Biochemistry 56*, 944-956.

[21] Piazza, M., Dieckmann, T., and Guillemette, J. G. (2018) *Front. Biosci. 23*, 1902-1922.

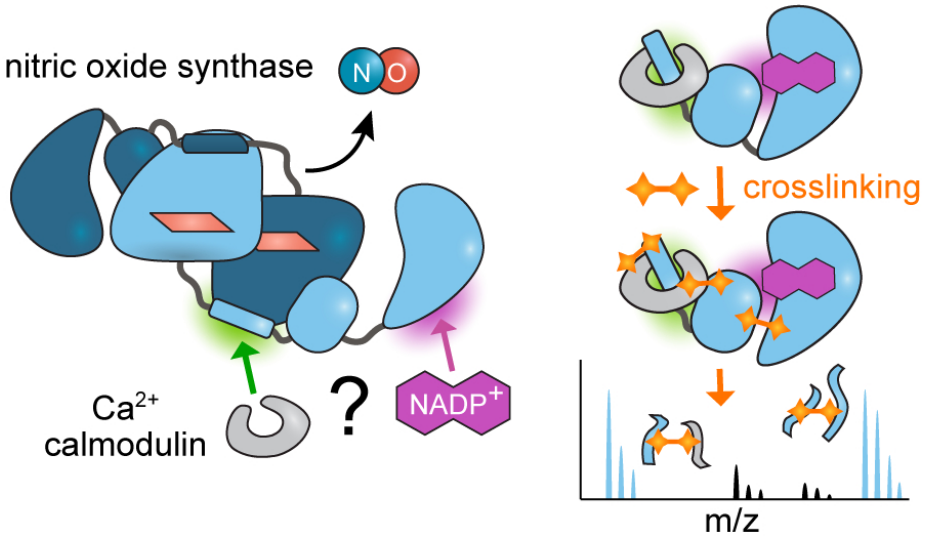


TOC "For Table of Contents use only"

82x44mm (300 x 300 DPI)